SMiRT-12 / K. Kussmaul (Editor)

K10/4

SEISMIC RESPONSE OF A NONSYMMETRIC NUCLEAR REACTOR BUILDING WITH A FLEXIBLE STEPPED FOUNDATION

H. Okano[1], A. Sakai[1], H. Takita[1], S. Fukunishi[2], T. Nakatogawa[2] and K. Kabayama[3]

[1]Kumagai-Gumi Co. Ltd., Tokyo, Japan
[2]Mutsubishi Atomic Power Industries, Inc., Tokyo, Japan
[3]Mitsubishi Heavy Industries, Ltd., Tokyo, Japan

SUMMARY

The effect of the nonsymmetry of a nuclear reactor building on its seismic response was studied. The nonsymmetric natures we considered, included the eccentricity of the superstructure and the nonsymmetry of the cross section of the foundation. A three-dimensional analysis which employed Green's function was applied to study the interaction between the soil and the nonsymmetrically sectioned foundation. The effect of a flexible foundation on its seismic response was also studied by applying the substructuring method, which combines the finite element method and Green's function method.

1. INTRODUCTION

Nuclear reactor buildings in Japan have adopted a regular structure to prevent the complex torsional vibration caused by earthquakes. However, an aseismic design which will permit a certain structural nonsymmetry may be required in future to increase the flexibility in planning nuclear power plants. The recent development of analysis methods has made it possible to study the effect of such nonsymmetry on the seismic response of a nuclear reactor building.

The nuclear reactor building, chosen for this study, has an eccentricity in its superstructure and step at the bottom of its foundation. To consider the effect of the eccentricity of the superstructure, the lumped-mass model, which has an independent center of the gravity and the rigidity for each floor, is used. The step at the bottom of a foundation not only effects its impedance functions but also its foundation input motion. The time delay in the arrival of the seismic wave to the bottom of the foundation causes a torsional foundation input motion. it is impossible to explain these phenomena by applying two-dimensional plane strain analysis or axisymmetric analysis. Therefore, we applied a three-dimensional Green's function method for the analysis of soil-structure interaction. Furthermore, the effect of foundation flexibility was also studied by the substructuring method, which combines the finite element method used to model the foundation and the Green's function method used to model the soil.

2. METHOD OF ANALYSIS

The dynamic substructuring method is usually employed for the three-dimensional soil-structure interaction analysis. The equation of motion by the substructuring method is given as follows:

$$[M]\begin{Bmatrix}\ddot{U}_S^t\\ \ddot{U}_F^t\end{Bmatrix}+\begin{bmatrix}K_{SS} & K_{SF}\\ K_{FS} & K_{FF}+K_F^*\end{bmatrix}\begin{Bmatrix}U_S^t\\ U_F^t\end{Bmatrix}=\begin{Bmatrix}0\\ F_F^*\end{Bmatrix} \quad (1)$$

where

$[M]$: Mass matrix of superstructure and foundation

$[K_{SS}]$, $[K_{SF}]$, $[K_{FS}]$, $[K_{FF}]$: Stiffness matrices of superstructure and foundation

$[K_F^*] = [\tilde{K}_F] - [K_F^e]$: Impedance matrix of ground remaining after excavation

$[\tilde{K}_F]$: Impedance matrix of unexcavated ground

$[K_F^e]$: Impedance matrix of excavated soil

The subscripts S and F denote nodes related to the superstructure and foundation. The superscript t denotes absolute displacement. $\{F_F^*\}$ on the righthand side of Eq. (1) is the driving force. The driving force corresponds to the seismic excitation force in general seismic response analyses, with the following form:

$$\{F_F^*\} = [\tilde{K}_F]\{\tilde{U}_F\} \tag{2}$$

where $\{\tilde{U}_F\}$ is the displacement field caused by an incident seismic wave in unexcavated ground. The impedance matrix of unexcavated ground $[\tilde{K}_F]$ was derived from Green's function obtained by point-load solution in thin layered medium[*1)], which satisfies the radiation condition. The impedance matrix of excavated soil was evaluated by the conventional finite element method.

If the foundation is considered to be rigid, the impedance matrix and the driving force are condensed as follows:

$$\begin{aligned} [K_F^{*}{}_0] &= [H]^T [K_F^*] [H] \\ \{F_F^{*}{}_0\} &= [H]^T \{F_F^*\} \end{aligned} \tag{3}$$

where

$\{U_F\} = [H]\{U_{F0}\}$: Displacement of each node of the rigid body.

$[H]$: Rigid deformation condition

$\{U_{F0}\} = (Ux, Uy, Uz, \Theta x, \Theta y, \Theta z)^T$: Representative displacement of the rigid body

The driving force is converted to the equivalent foundation input motion, given as follows:

$$\{U_F^{*}{}_0\} = [K_F^{*}{}_0]^{-1}\{F_F^{*}{}_0\} \tag{4}$$

The foundation input motion is the seismic response of a rigid massless foundation.

3. MODEL DESCRIPTIONS

The nuclear reactor building, chosen for this study, has an eccentricity in its superstructure and a step at the bottom of its foundation. Table 1 shows the parameters of the analyses. For comparison, the case without superstructure eccentricity and that without foundation step are also analyzed. To consider the effect of the superstructure eccentricity, the lumped-mass model which has independent nodes for center of gravity and rigidity, is used. They are connected to each other by a rigid beam element. The properties of each layer are evaluated as a three-dimensional beam element. Fig. 1 shows the analytical model of the superstructure. The ratio of eccentricity is less than 15% in the X-direction and less than 10% in the Y-direction. Figs. 2 and 3 show the analytical models of the rigid foundations and flexible foundation, respectively. The step depth is 6 meters (CASE-3 and CASE-4). The step plan of step is mainly nonsymmetric with respect to the X-axis. In all cases, the supporting ground is assumed to be uniform hard rock, and an artificial ground motion is used for the seismic response analyses.

4. ANALYTICAL RESULTS

4.1 Rigid Foundation Model

The main components of impedance functions of the rigid foundations, obtained from Eq. (3), are shown in Fig. 4. The real and imaginary parts of the stepped foundation (CASE 3) are slightly larger than those with no step (CASE 2). These tendencies are the same as those generally observed in embedded foundations. Figs. 5 and 6 show the foundation input motions when the foundation is subjected to earthquake motion in the X-direction, and in the Y-direction, respectively. The foundation input was normalized with respect to the amplitude of the free field at the surface. The rocking component was multiplied by the depth of the step, and the torsional component was multiplied by an equivalent radius. As in the case of symmetric embedded foundations, the horizontal component of input motion decreases and the rocking component increases as the frequency increases. One characteristic of the stepped foundation is that the foundation input motion had a torsional component, because vertically incident waves did not arrive simultaneously at the bottom of foundation. This component increases as the frequency increases. The torsional foundation input motion was larger in the case when the structure was subjected to earthquake motion in the X-direction than in the case when the structure subjected to such motion in the Y-direction, because the plan of the step of foundation is mainly nonsymmetric with respect to the X-axis.

Fig. 7 shows the maximum responses of displacement and acceleration when the structure was subjected to earthquake motion in the X-direction. Figs. 8 and 9 show the response spectra at the center of rigidity and the floor response spectra taking the torsional effect into consideration, respectively. Although a significant amount of the torsional foundation input motion is induced in those cases, remarkable differences are not observed in those results.

Figs. 10～12 show the maximum responses and the response spectra when the structure was subjected to earthquake motion in the Y-direction. These figures indicate that the floor response spectra taking the torsional effect into consideration, is slightly effected by nonsymmetries of the structure in a short period region, although the maximum responses and response spectra at the center of rigidity are not effected. Those difference are considered to be caused by the eccentricity of the superstructure, because the eccentricity of the superstructure is relatively large and the torsional foundation input motion is small in those cases.

4.2 Flexible Foundation Model

The effect of foundation flexibility is also studied because a machinery room is located in the step of foundation of the reactor building chosen for this study. The FEM model of the foundation, which is shown in Fig. 3, employs eight node solid elements and thin shell elements. The bottom nodes of the superstructure and the corresponding nodes of the foundation were connected by a multi point constraint method.

Fig. 13 shows the maximum response of displacement and acceleration when the structure was subjected to earthquake motion in the Y-direction. This figure suggests that the effect of foundation flexibility on maximum responses is negligible. Figs. 14 and 15 show the floor response spectra of the center of rigidity and the floor response spectra taking the torsional effect into account. In the short period region, slight differences are observed, but effects of the foundation flexibility are not significant.

5. CONCLUSIONS

Following results were obtained, from the analytical studies mentioned above.

(1) The superstructure eccentricity does not effect either the maximum response or the response spectra of the center of rigidity, but it slightly effects the floor response spectra taking the torsional effect into consideration in a short period region. However, the effect of eccentricity on floor response spectra is not significant from an engineering point of view as long as ratio of eccentricity is less than 15%.

(2) Although the step at the bottom of the foundation induced torsional input motion, the effect on seismic response is smaller than the effect of superstructure eccentricity, as long as the depth of the step is less than 6 meters.

(3) The effect of the foundation flexibility was not significant, although the flexibility slightly affects on the floor response spectra in the short period region.

REFERENCE

1) H.Tajimi and M.Izumikawa, "Dynamic Analysis of Embedded Mat Foundations by Application of Point-Load Solution in a Thin Layered Medium", Proc. of the Sixth Japan Earthquake Engineering Symposium (in Japanese), pp1745-1752, 1982.

Table 1 Parameters of Analyses

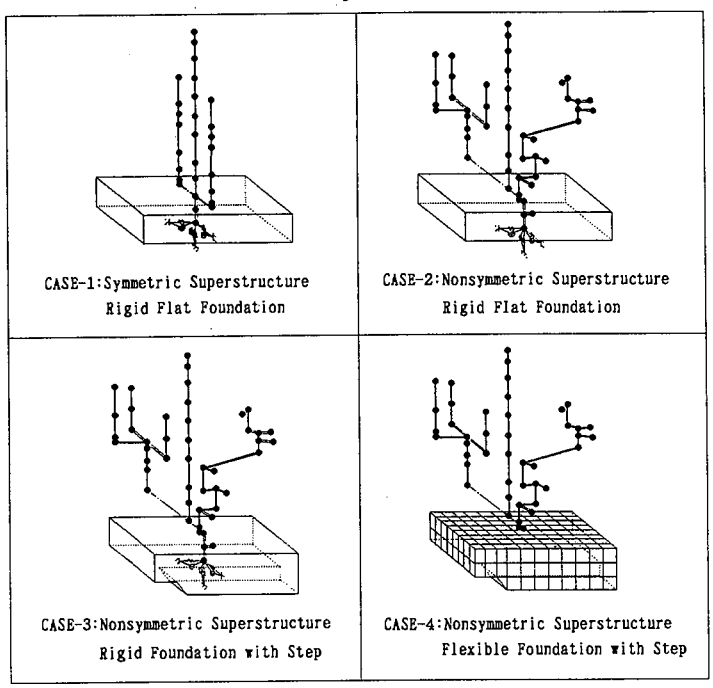

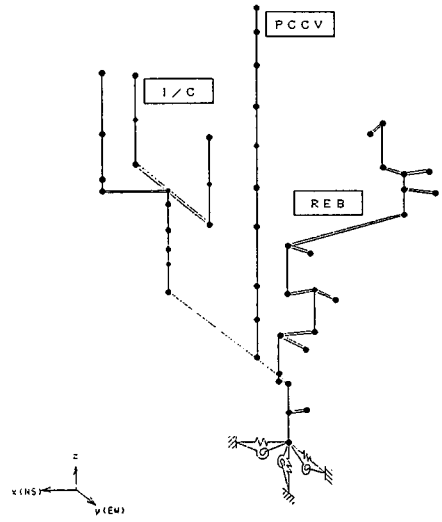

Fig. 1 Lumped Mass Model of Superstructure

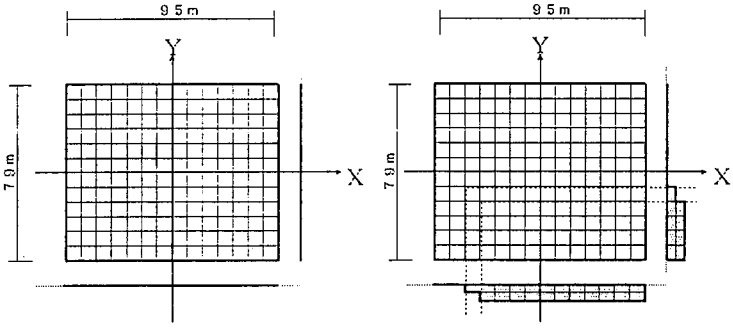

(a) Flat Foundation (b) Stepped Foundation

Fig. 2 Analysis Model of Rigid Foundation

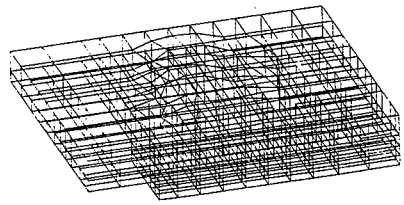

Fig. 3 FEM Model of Flexible Foundation

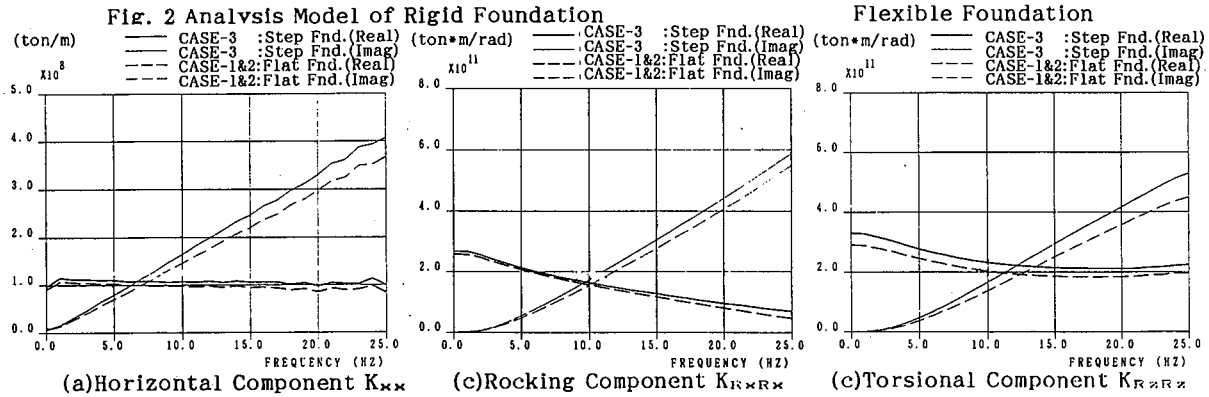

(a)Horizontal Component K_{xx} (c)Rocking Component $K_{R_xR_x}$ (c)Torsional Component $K_{R_zR_z}$

Fig. 4 Impedance Function of Rigid Foundations

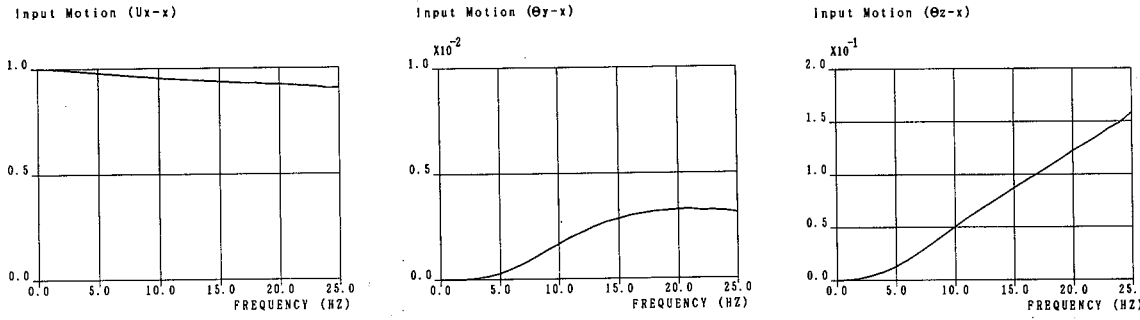

(a)Horizontal Component (b)Rocking Component (c)Torsional component

Fig. 5 Input Motion of Stepped Foundation: Subjected to Earthquake in X-Direction

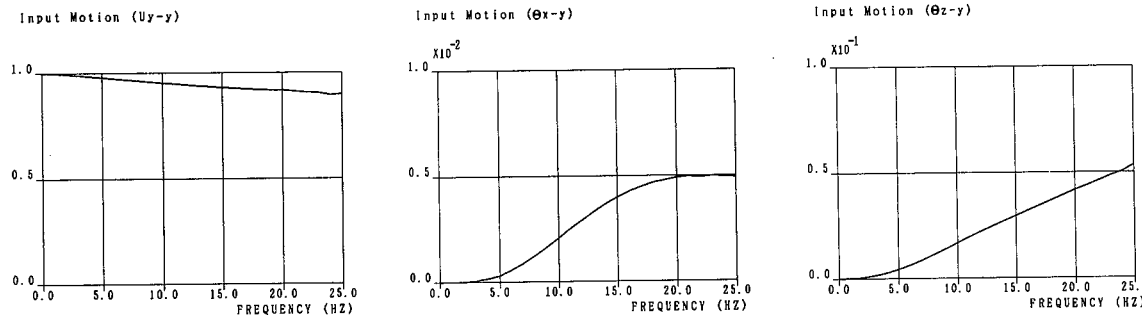

(a)Horizontal Component (b)Rocking Component (c)Torsional Component

Fig. 6 Input Motion of Stepped Foundation: Subjected to Earthquake in Y-Direction

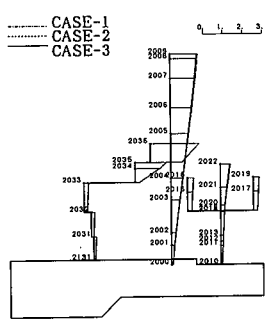

(a) Maximum Displacement

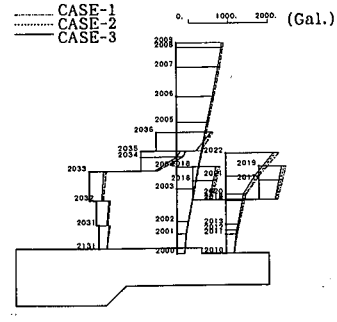

(b) Maximum Acceleration

Fig. 7 Maximum Response: Subjected to Earthquake In X-Direction

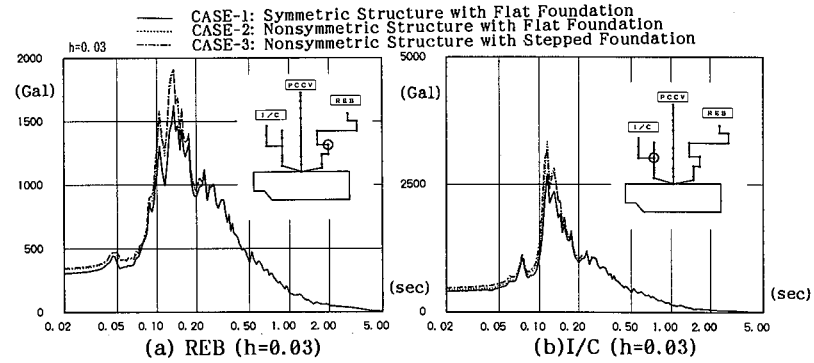

(a) REB (h=0.03) (b)I/C (h=0.03)

Fig. 8 Response Spectra at the Center of Rigidity: Subjected to Earthquake In X-Direction

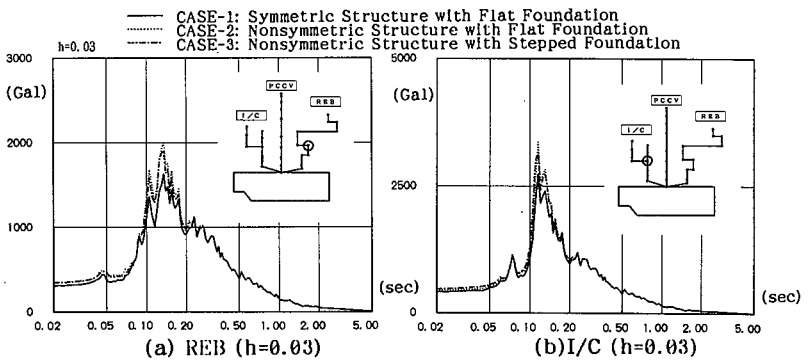

(a) REB (h=0.03) (b)I/C (h=0.03)

Fig. 9 Floor Response Spectra taking Torsional Effect into consideration: Subjected to Earthquake in X-Direction

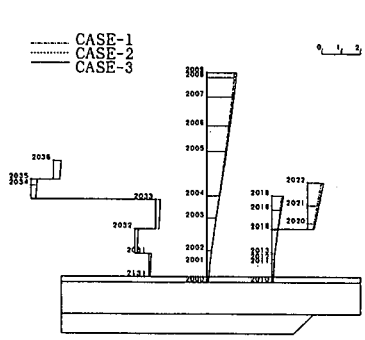

(a) Maximum Displacement

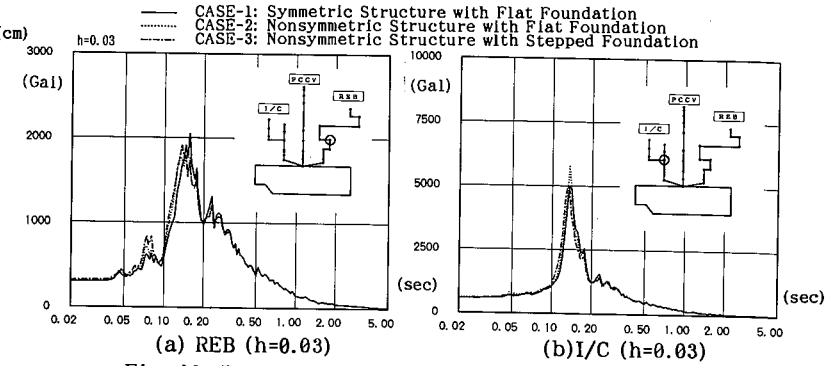

(a) REB (h=0.03) (b)I/C (h=0.03)

Fig. 11 Response Spectra at the Center of Rigidity: Subjected to Earthquake In Y-Direction

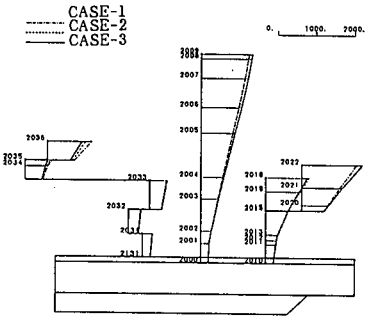

(b) Maximum Acceleration

Fig. 10 Maximum Response: Subjected to Earthquake In Y-Direction

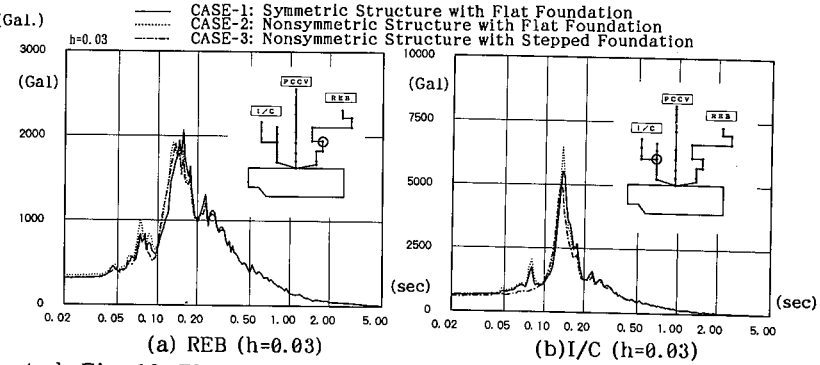

(a) REB (h=0.03) (b)I/C (h=0.03)

Fig. 12 Floor Response Spectra taking Torsional Effect into consideration: Subjected to Earthquake in Y-Direction

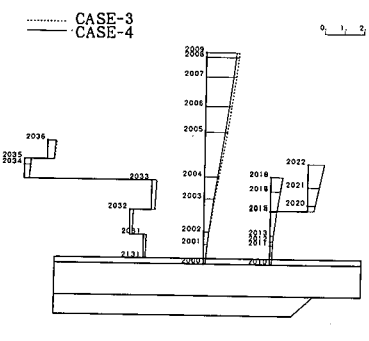

(a) Maximum Displacement

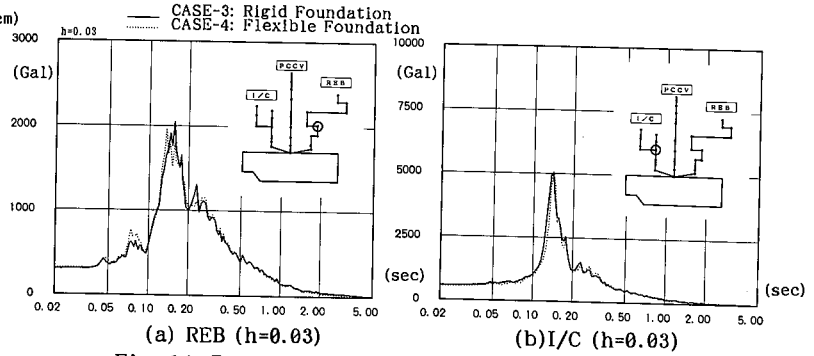

(a) REB (h=0.03) (b)I/C (h=0.03)

Fig. 14 Response Spectra at the Center of Rigidity: Subjected to Earthquake In Y-Direction

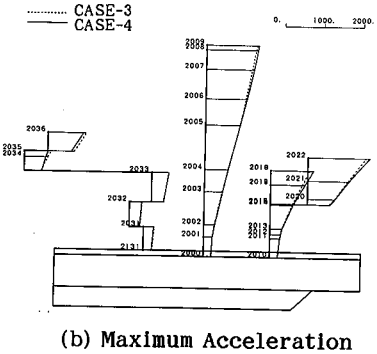

(b) Maximum Acceleration

Fig. 13 Maximum Response: Subjected to Earthquake In Y-Direction

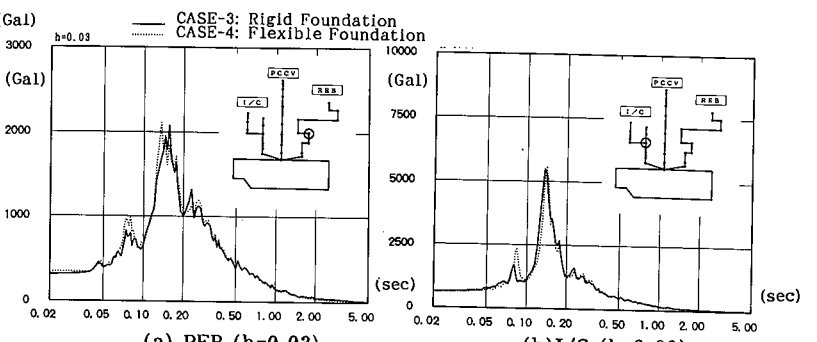

(a) REB (h=0.03) (b)I/C (h=0.03)

Fig. 15 Floor Response Spectra taking Torsional Effect into consideration: Subjected to Earthquake in Y-Direction